ELECTROSPINNING OF HYDROXYAPATITE-GELATINE SCAFFOLDS: PHYSICAL CHARACTERISATION AND PROCESS OPTIMISATION

A. A. Salifu[1], C. Lekakou[1]*

[1] *Division of Mechanical, Medical and Aerospace Engineering, Faculty of Engineering and Physical Sciences, University of Surrey, Guildford, Surrey GU2 7XH, UK.*
**Email: C.Lekakou@surrey.ac.uk*

Keywords: Electrospinning; Gelatine; Hydroxyapatite (HA); Bone Tissue Engineering.

Abstract
Electrospun scaffolds of hydroxyapatite-gelatine nanocomposites were fabricated, crosslinked and subjected to image analysis, water swelling and mechanical testing. Fibre diameter and pore size of scaffolds increased with the applied voltage and the hydroxyapatite (HA) content. The scaffolds were stable in water for up to three weeks and there was a positive correlation between their mechanical properties and the applied voltage and the HA content. Maximum Young's modulus and tensile strength of 925 MPa and 9.75 MPa, respectively, were recorded for 25% HA scaffold.

1 Introduction

Bone extracellular matrix (ECM) is a nanocomposite of hydroxyapatite (HA) crystals and a fibrous collagen matrix [1]; the nanoscale interaction of these components gives bone its unique mechanical properties [2]. Therefore, electrospun hydroxyapatite-collagen (and gelatine) scaffolds can serve as 3D templates for *in vitro* bone tissue formation: the scaffolds mimic the structure and function of the native ECM of bone, thereby replacing the native ECM until the bone cells regenerate a new matrix. Electrospun HA-gelatine and HA-collagen scaffolds have been designed by various researchers and have been shown to favour *in vitro* bone formation compared to synthetic polymer composites such as PCL/HA and PLLA/HA [3] [4], owing to the lack of cell-recognition signals in the synthetic polymers for cell attachment [5]. Furthermore, in a study by Kim *et al.* (2005) [6], it was shown that nanocomposite HA-gelatine scaffolds fabricated via *in situ* precipitation of HA within the gelatine matrix improved *in vitro* osteogenesis compared to conventionally mixed HA-gelatine scaffolds. The nanocomposites increased ionic release and serum protein adsorption, thereby improving cell attachment. Therefore, electrospinning these nanocomposites into nanofibrous scaffolds that mimic the bionanostructure of the native bone ECM should further enhance bone tissue formation, yet this has not been adequately pursued.

Scaffold properties such as fibre diameter and pore size have been shown to affect *in vitro* bone formation. Pore size is predominantly controlled by the fibre diameter; the pore size enlarges when the fibre diameter is increased [7]. Thus, scaffolds with larger fibre diameters are expected to have larger pore sizes. Larger pores allow effective diffusion of nutrients to

the cells as they migrate into the scaffold. They also enhance the removal of cell metabolic waste substances that can be become cytotoxic if they build up in the scaffold. Hence, larger fibre diameters and larger pore sizes enhance cell proliferation and migration as observed in studies on the effect of electrospun PLLA scaffold fibre diameter (140 – 2100 nm) on MC3T3-E1 mouse osteoblast cells [8]; the effect of electrospun gelatine scaffold fibre diameter (110 nm and 610 nm) and pore size (1 μm^2 and 10.7 μm^2) on MG63 osteoblast cells [9]; and the effect of gelatine scaffold pore size (50 – 500 μm) on rat articular chondrocytes [10]. However, little is known about the effects of fibre diameter and pore size on *in vitro* osteoblast proliferation and bone tissue formation on electrospun HA-gelatine nanocomposite scaffolds. Electrospun HA-gelatine scaffolds with varying fibre diameters and pore sizes can be fabricated by varying electrospinning processing conditions such as the applied voltage and the HA content of the nanocomposites.

This study aims to investigate the effects of applied voltage and HA content on the resulting fibre diameters and pore sizes of electrospun scaffolds of HA-gelatine nanocomposites prepared via *in situ* HA precipitation, in order to optimise scaffold characteristics such as the water stability and mechanical strength that are crucial for osteogenesis and eventual integration with existing bone at defect sites.

2 Materials and Methods

The following materials were obtained from Sigma-Aldrich (Gillingham, UK): phosphoric acid, calcium hydroxide, 2,2,2-trifluoroethanol (TFE), glutaraldehyde (grade II, 25% in water) and Gelatine Type A (porcine skin, 300 Bloom). Sodium hydroxide was obtained from Fisher Scientific (Loughborough, UK).

2.1 Preparation of Hydroxyapatite-Gelatine Nanocomposites

Hydroxyapatite (Ca/P ratio 1.67) was produced from the following reaction between calcium hydroxide and phosphoric acid: $10\ Ca(OH)_2 + 6\ H_3PO_4 \rightarrow Ca_{10}(PO_4)_6(OH)_2 + 18\ H_2O$. The following nanocomposite compositions were prepared: 10, 20, 25, 30 and 40 wt% HA. The amounts of calcium hydroxide, phosphoric acid and gelatine used are shown in Table 1. Gelatine powder was added to the $Ca(OH)_2$ solution and stirred at about 37 °C for 1 hour. Drops of H_3PO_4 solution were subsequently added to the $Ca(OH)_2$ – gelatine solution to precipitate the HA nanoparticles within the gelatine sol and the pH of the resulting solution was adjusted to approximately 10 by adding drops of 1M NaOH solution. The HA was allowed to age/mature for 24 hours at 37 °C. The samples were frozen at -20 °C for approximately 48 hours followed by freeze-drying under vacuum at -40 °C for a further 48 hours.

2.2 Electrospinning and Crosslinking

The set-up used for electrospinning is shown in Figure 1. Pure gelatine and HA-gelatine were dissolved in 2,2,2-trifluoroethanol (TFE) at a concentration of 10% w/v. Each solution was loaded into a 5 mL syringe with an 18 gauge blunt end needle at its tip. A syringe pump (Cole-Parmer, Vernon Hills, IL, USA) was used to deliver each solution at a constant feed rate of 5 mL/h followed by the application of high voltage (20 kV, 25 kV and 30 kV) from a high voltage power supply (Glassman High Voltage, Inc., Whitehouse Station, NJ, USA) to the solutions. The distance between the tip of the needle and the 30 rpm rotating wire-framed

collector was maintained at 15 cm. The electrospinning experiment was carried out at room temperature, atmospheric air and humidity for approximately 2 hours and the resulting fibre mats were air dried on the collector for 24 hours after which they were carefully removed and crosslinked in a sealed desiccator containing saturated glutaraldehyde vapour for durations of 2 hours and 4 hours.

HA/(Gel-HA) [wt%]	Amount of $Ca(OH_2)$ [g/25 mL]	Amount of H_3PO_4 [g/25 mL]	Amount of Gelatine [g]
10	0.5041	0.4000	6.1506
20	1.0081	0.8000	5.4672
25	1.2600	1.0000	5.1256
30	1.5120	1.2000	4.7838
40	2.0161	1.6000	4.1006

Table 1. The amounts of calcium hydroxide, phosphoric acid and gelatine used to prepare different compositions of HA-gelatine nanocomposites.

2.3 Scanning Electron Microscopy (SEM) and Image Analysis

The samples were sputter coated with 30 nm of gold/palladium mixture (Au/Pd; 60:40) and their morphologies observed under a Hitachi S-3200N Scanning Electron Microscope at 15 kV. The distribution of fibre diameters and pore sizes was determined, by measuring 125 fibres and 75 pores respectively, with the aid of an image analysis software (Digimizer® v4.0.0, MedCalc Software, Belgium).

2.4 Water Swelling Test

The dry weights, W_d, of crosslinked scaffolds were recorded and they were fully immersed in deionised water and incubated at 37 °C. The swollen weights, W_s, were measured every day for 3 weeks and their water swelling ratios determined as $(W_s - W_d)/ W_d$.

2.4.3 Mechanical Testing

Tensile stress – tensile strain curves of the dry scaffolds (13 mm x 3 mm) were generated using an Instron 5500R 6025 Testing Machine, with a 10 N load cell, under a crosshead speed of 1 mm/min. For each scaffold, tests were performed in the same direction as the direction of fibre collection (circumferential direction on the rotating wired-drum collector in electrospinning) and also at 90^o to the direction of fibre collection (axial direction).

3 Results and Discussion

3.1 Electrospun Scaffolds

The hydroxyapatite-gelatine nanocomposites with 30% and 40% HA could not be spun into fibres. Increasing the composite solution concentration up to 30% w/v (in TFE) did not improve electrospinnability. Figure 2 reports on the morphological differences between the uncrosslinked and crosslinked scaffolds of 10% HA spun at 20 kV. The fibre alignment in the uncrosslinked scaffolds was poor which may be attributed to the low speed of rotation of the collector (30 rpm) used in this study. To improve fibre alignment, an optimum rate of rotation

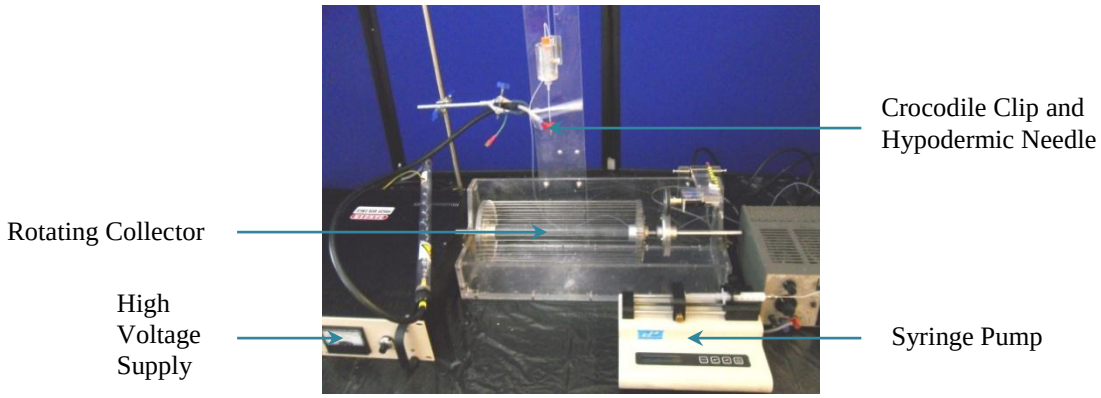

Figure 1. The electrospinning set-up

is required to counterbalance the rates of fibre formation and fibre collection. Figure 2(b) reveals the arrangement of fibres in a crosslinked network. Fibre crosslinking was achieved after only 2 hours exposure to glutaraldehyde even though there was a slight increase in fibre entanglements when crosslinking time was increased to 4 hours. Generally, there were some beads along the fibres. As shown in Figure 3, there was little beading in pure gelatine scaffolds compared to their HA-gelatine counterparts. The beads in the nanocomposite scaffolds were mainly HA particles that were distributed along the lengths of gelatine fibres. The diameters of these fibres, with their embedded HA particles, were in the nanoscale, which indicated that nanocomposites of HA and gelatine were, indeed, fabricated.

3.2 Fibre Diameter

There was a decline in the scaffold average fibre diameters when the applied voltage and the HA content were increased, as illustrated in Figure 4. Pure gelatine fibres had about three times larger average fibre diameters in relation to the applied voltage, followed by 10% HA, 20% HA and 25% HA fibres. An increase in the applied voltage leads to a greater charge repulsion in the fibre jet coupled with a stronger electric field, giving rise to a greater fibre stretching before deposition and culminating in a reduction in the fibre diameter [11] [12]. Successful electrospinning relied on the viscoelastic forces of the polymeric gelatine resisting fibre jet stretching. Thus, increasing the HA content from 0% (pure gelatine) to 25% decreased the gelatine content in the nanocomposites, which meant that there was less resistance to fibre stretching leading to a reduction in the fibre diameter. Changes in the average fibre diameter were more pronounced in relation to variations in the HA content than for the applied voltage. For instance, the average range of fibre diameters across all scaffolds with respect to the applied voltage was 180 ± 57 nm whereas that for the HA content was 1135 ± 66 nm, representing a six-fold increase. This shows that varying the HA content of the scaffolds can produce larger changes in fibre diameters than the applied voltage.

3.3 Pore Size

Similarly, the average pore area decreased, albeit slightly, with increasing applied voltage and HA content; and there was an approximate six-fold increase in pure gelatine's average pore area compared to the nanocomposite scaffolds, as shown in Figure 5. As previously observed, increases in the applied voltage and the HA content decrease the fibre diameter and smaller diameter fibres are expected to pack more tightly in the scaffolds than larger diameter fibres,

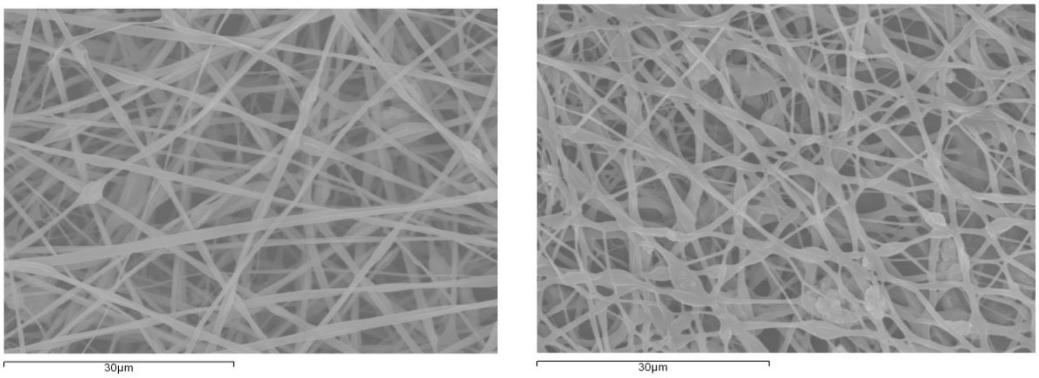

Figure 2. SEM micrographs of (a) uncrosslinked and (b) crosslinked 10% HA nanocomposite fibres electrospun at 20 kV.

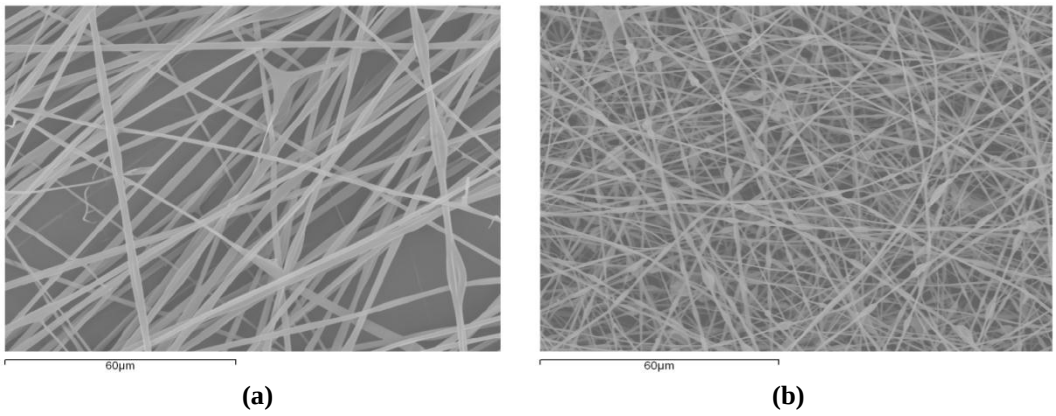

Figure 3. SEM micrographs of (a) pure gelatine and (b) 25% HA nanocomposite fibres electrospun at 20 kV.

leading to smaller pore sizes. This observation is consistent with a study by Soliman *et al.* (2010) [13] on the effect of fibre diameter and packing density on the pore sizes of electrospun PCL scaffolds. They found out that the pore size was mainly dependent on the fibre diameter and packing density. Scaffolds with larger fibre diameters gave rise to larger pore sizes and vice versa. Conversely, a lower packing density led to a larger pore size. Increasing the duration for fibre crosslinking from 2 hours to 4 hours resulted in a decrease in the average pore areas across all scaffolds as more reactions occurred between glutaraldehyde's aldehyde groups and gelatine's amino groups along the lengths of the fibres, giving rise to more crosslinkages.

3.4 Water Stability

Crosslinking markedly improved the structural integrity of the scaffolds versus the uncrosslinked samples whose structures were immediately distorted upon contact with water. All the crosslinked scaffolds absorbed water and remained stable in the 37 °C aqueous environment. However, towards the end of three weeks, the scaffolds appeared relatively weak, with the 2 hour-crosslinked samples appearing even weaker than the 4 hour-crosslinked ones probably because of the presence of free or degraded de-crosslinked fibres in the scaffolds. Figure 6 tracks the water swelling ratios of 25% HA scaffolds for 3 weeks.

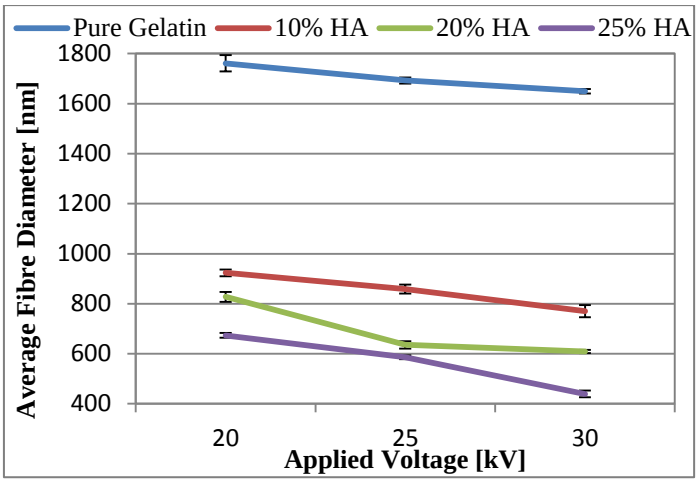

Figure 4. Average fibre diameter against applied voltage for different scaffolds.

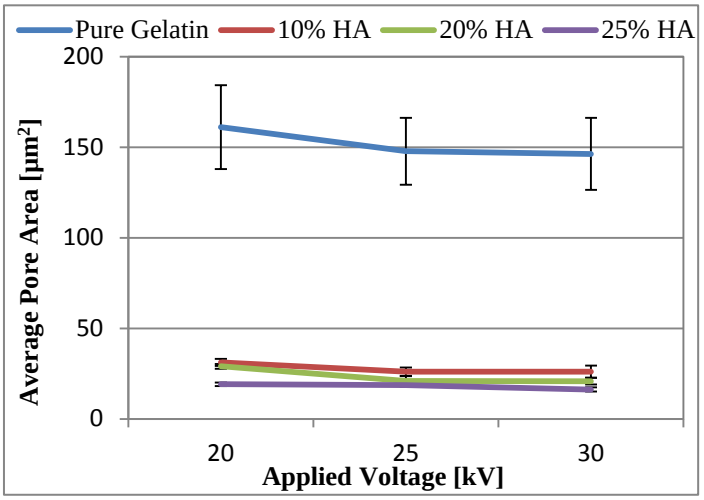

Figure 5. Average pore area against applied voltage for different scaffolds.

The ratios increased sharply for the first 24 hours of soaking and remained approximately constant for the next 3 days, as the scaffolds became saturated with water. They then declined substantially by day 10 and gradually decreased afterwards until day 21 as a result of scaffold degradation. The gelatine content, which is responsible for the water absorption, decreases as the scaffolds degrade leading to a decrease in the swelling ratios. This shows that the scaffolds produced in this study could withstand the aqueous environment required for osteoblast growth and bone tissue formation. However, the scaffolds degraded with time and so the commencement of bone tissue production to replace the degrading scaffold and maintain the structural integrity of the extracellular environment should not exceed 3 weeks.

3.5 Mechanical Properties

Generally, the tensile strengths and Young's moduli of 25% HA scaffolds were higher than the others, as illustrated in Figure 7, due to the increased HA content and the decreased fibre diameter and pore size. Also, the Young's modulus of all scaffolds increased as the applied voltage increased, irrespective of the crosslinking time and the direction of tensile loading. Tensile loading in the circumferential direction of the drum collector gave rise to higher Young's moduli and tensile strengths than in the axial direction of the drum collector, which confirmed that more fibres were aligned in the circumferential direction of the drum collector.

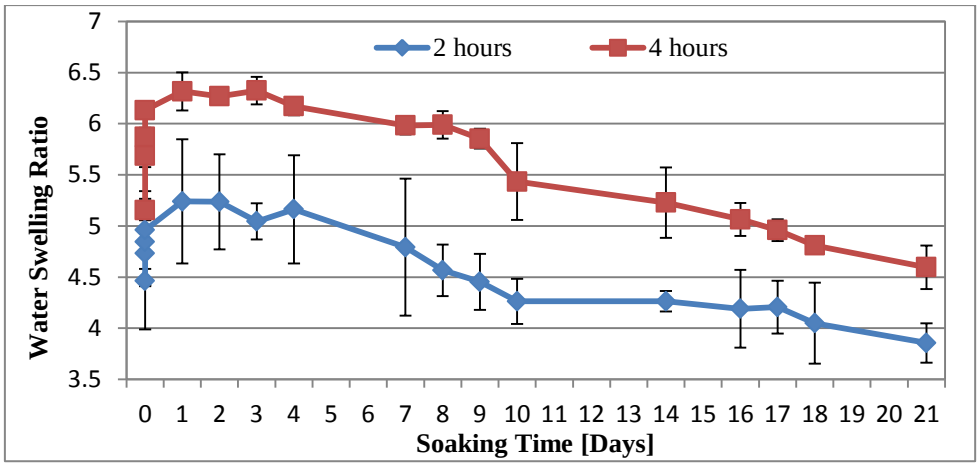

Figure 6. Water swelling ratios of 25% HA scaffolds over 3 weeks soaking in water at 37 °C.

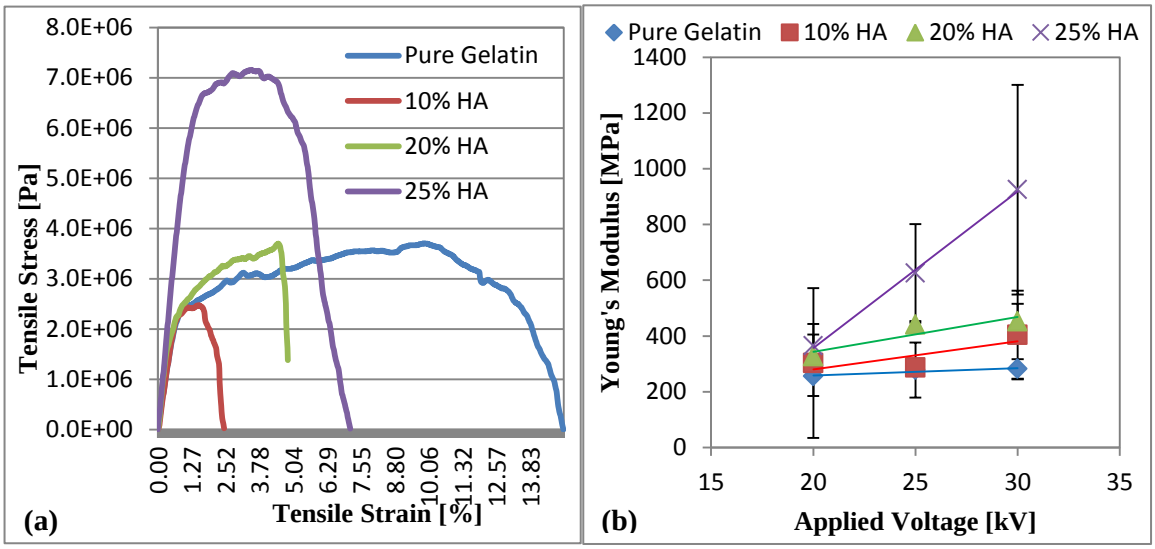

Figure 7. (a) Typical stress – strain curves; (b) Young's modulus against applied voltage for different scaffolds.

In addition, the mechanical properties of the scaffolds improved as the crosslinking time was increased from 2 to 4 hours, owing to the reduction in pore size. The scaffolds produced in this study exhibited maximum values of 925 MPa and 9.75 MPa for Young's modulus and tensile strength, respectively, corresponding to 25% HA. These values were much lower than the tensile properties of human femur compact bone (17.6 GPa and 124 MPa respectively [14]). Nonetheless, these scaffolds could be very useful in non-weight bearing defect sites. Maximum Young's moduli reported in other studies on HA-gelatine nanocomposite scaffolds include: 48.3 MPa [15], 60 MPa [16] and 412 MPa [17], which were much lower than the values reported in this study. A better degree of HA nanoparticle distribution within the gelatine matrix as well as the extent of crosslinking could have been responsible for the improved mechanical properties of the present study.

4 Conclusions

Nanocomposites of hydroxyapatite-gelatine were fabricated and electrospun. Image analysis showed that scaffold fibre diameter and pore size increased in response to increases in either the applied voltage or the HA content. It was also demonstrated that varying the HA content rather than the applied voltage was more effective in controlling fibre diameter. The scaffolds were stable in water for up to three weeks and their mechanical properties were dependent on

the fibre diameter and pore size as well as the direction of loading. In all, the 25% HA scaffold exhibited the best properties for supporting bone tissue engineering. This study demonstrates that scaffold properties can be tailored towards optimal bone tissue formation.

5 References

[1] Murphy W.L., Simmons C.A., Kaigler D., Mooney D.J. Bone regeneration via a mineral substrate and induced angiogenesis. *J Dent Res*, **83,** 204-210 (2004).
[2] Taton T.A. Boning up on biology. *Nature*, **412**, 491-492 (2001).
[3] Venugopal J., Low S., Choon A.T., Barath Kumar A.B., Ramakrishna S. Nanobioengineered electrospun composite nanofibres and osteoblasts for bone regeneration. *Artificial Organs*, **32**, 388-397 (2008).
[4] Prabhakaran M.P., Venugopal J., Ramakrishna S. Electrospun nanostructured scaffolds for bone tissue engineering. *Acta Biomaterialia*, **5**, 2884-2893 (2009).
[5] Kim B.S., Mooney D.J. Development of biocompatible synthetic extracellular matrices for tissue engineering. *Trends Biotechnol*, **16,** 224-230 (1998).
[6] Kim H.W., Kim H.E. Salih V. Simulation of osteoblast responses to biomimetic nanocomposites of gelatin-hydroxyapatite for tissue engineering scaffolds. *Biomaterials*, **26**, 5221-5230 (2005).
[7] Eichhorn J.S., Sampson W.W. Statistical geometry of pores and statistics of porous nanofibrous assemblies. *J Royal Soc Interface*, **2**, 309-318 (2005).
[8] Badami A.S., Kreke M.R., Shane Thompson M., Riffle J.S., Goldstein A.S. Effect of fibre diameter on spreading, proliferation and differentiation of osteoblastic cells on electrospun poly(lactic acid) substrates. *Biomaterials*, **27**, 596-606 (2006).
[9] Sisson K., Zhang C., Farach-Carson M.C., Bruce Chase D., Rabolt J.F. Fibre diameters control osteoblastic cell migration and differentiation in electrospun gelatin. *J Biomed Mater Res A*, **94A**, 1312-1320 (2010).
[10] Lien S.M., Ko L.Y., Huang T.J. Effect of pore size on ECM secretion and cell growth in gelatin scaffold for articular cartilage tissue engineering. *Acta Biomaterialia*, **5**, 670-679 (2009).
[11] Lee J.S., Choi K.H., Ghim H.D., Kim S.S., Chun D.H., Kim H.Y., Lyoo W.S. Role of molecular weight of atactic poly(vinyl alcohol) (PVA) in the structure and properties of PVA nanofabric prepared by electrospinning. *J Appl Polym Sci*, **93,** 1638-1646 (2004).
[12] Megelski S., Stephens J.S., Chase D.B., Rabolt J.F. Micro- and nanostructured surface morphology on electrospun polymer fibres. *Macromolecules*, **35,** 8456-8466 (2002).
[13] Soliman S., Sant S., Nichol J.W., Khabiry M., Traversa E., Khademhosseini A. Controlling the porosity of fibrous scaffolds by modulating the fibre diameter and packing density. *J Biomed Mater Res A*, **96A**, 566-574 (2011).
[14] Fung Y.C. *Biomechanics: Mechanical Properties of Living Tissues, 2nd Edition.* Springer-Verlag, New York (1993).
[15] Azami M., Rabiee M., Mostarzadeh F. Glutaraldehyde crosslinked gelatin/hydroxyapatite nanocomposite scaffold engineered via compound techniques. *Polymer Composites*, **31,** 2112-2120 (2010).
[16] Salifu A.A., Nury B.D., Lekakou C. Electrospinning of nanocomposite fibrillar tubular and flat scaffolds with controlled fibre orientation. *Ann Biomed Eng*, **39**, 2510-2520 (2011).
[17] Kim H.W., Song J.H., Kim H.E. Nanofibre generation of gelatin-hydroxyapatite biomimetics for guided tissue regeneration. *Adv Funct Mater*, **15**, 1988-1994 (2005).